Fionnuala B. Hickey,[1,2,3] James B. Corcoran,[1,2] Brenda Griffin,[1,4] Una Bhreathnach,[1,2] Heather Mortiboys,[5] Helen M. Reid,[4] Darrell Andrews,[1,4] Shane Byrne,[1,4] Fiona Furlong,[6] Finian Martin,[1,4] Catherine Godson,[1,2] and Madeline Murphy[1,2]

# IHG-1 Increases Mitochondrial Fusion and Bioenergetic Function

*Diabetes 2014;63:4314–4325 | DOI: 10.2337/db13-1256*

**Induced in high glucose-1 (IHG-1) is a conserved mitochondrial protein associated with diabetic nephropathy (DN) that amplifies profibrotic transforming growth factor (TGF)-β1 signaling and increases mitochondrial biogenesis. Here we report that inhibition of endogenous IHG-1 expression results in reduced mitochondrial respiratory capacity, ATP production, and mitochondrial fusion. Conversely, overexpression of IHG-1 leads to increased mitochondrial fusion and also protects cells from reactive oxygen species–induced apoptosis. IHG-1 forms complexes with known mediators of mitochondrial fusion—mitofusins (Mfns) 1 and 2—and enhances the GTP-binding capacity of Mfn2, suggesting that IHG-1 acts as a guanine nucleotide exchange factor. IHG-1 must be localized to mitochondria to interact with Mfn1 and Mfn2, and this interaction is necessary for increased IHG-1–mediated mitochondrial fusion. Together, these findings indicate that IHG-1 is a novel regulator of both mitochondrial dynamics and bioenergetic function and contributes to cell survival following oxidant stress. We propose that in diabetic kidney disease increased IHG-1 expression protects cell viability and enhances the actions of TGF-β, leading to renal proximal tubule dedifferentiation, an important event in the pathogenesis of this devastating condition.**

Induced in high glucose-1 (IHG-1), also known as tRNA-histidine guanylyltransferase 1-like, was originally identified as a glucose-regulated transcript in a screen for genes associated with diabetic nephropathy (DN) (1–3). IHG-1 is a highly conserved protein localized to mitochondria and plays an important regulatory role in mitochondrial biogenesis by stabilizing the transcriptional cofactor peroxisome proliferator–activated receptor-γ coactivator 1α (PGC-1α) (4). IHG-1 expression is increased in human DN and is likely to contribute to the development of tubulointerstitial fibrosis (TIF) in this disease (5). IHG-1 amplifies responses to the major fibrotic mediator transforming growth factor (TGF)-β1 by both increasing and prolonging phosphorylation of signal mediator Smad3 (5). IHG-1 must be localized to mitochondria to amplify TGF-β1 signaling (6).

Mitochondria play a central role in cellular adaptation to hyperglycemic conditions (7). In diabetes, increased glucose metabolism resulting in increased mitochondrial production of reactive oxygen species (ROS) is believed to be the primary event leading to the development and progression of diabetic vascular complications (8). Oxidant stress resulting from increased ROS contributes to TGF-β1 activity in the diabetic kidney (9,10). Hyperglycemia, oxidative stress, and TGF-β1 signaling induce increased mitochondrial biogenesis and alterations in mitochondrial dynamics (11–17). Mitochondria are plastic organelles that frequently change shape and size. Dynamic fusion and fission events are important for the bioenergetic function of mitochondria (18) as is PGC-1α activity, which plays a key role in enhancing mitochondrial stress–related bioenergetic function (19).

[1]Diabetes Complications Research Centre, Conway Institute, University College Dublin, Belfield, Dublin, Ireland
[2]School of Medicine and Medical Sciences, University College Dublin, Belfield, Dublin, Ireland
[3]Trinity Health Kidney Centre, Trinity College, Dublin, Ireland
[4]School of Biomolecular and Biomedical Science, University College Dublin, Belfield, Dublin, Ireland
[5]Academic Neurology Unit, Medical School, University of Sheffield, Sheffield, U.K.
[6]School of Pharmacy, Queen's University Belfast, Belfast, Northern Ireland
Corresponding author: Madeline Murphy, madeline.murphy@ucd.ie.

Received 15 August 2013 and accepted 2 July 2014.
This article contains Supplementary Data online at http://diabetes.diabetesjournals.org/lookup/suppl/doi:10.2337/db13-1256/-/DC1.
C.G. and M.M. share equivalent seniority.

Mitochondrial fusion relies on dynamin-related GTPases, mitofusins (Mfns) 1 and 2, and optic atrophy 1 (OPA1) (20,21). Mitochondrial fission relies on another GTPase: cytosolic dynamin-related protein 1 (Drp1), which translocates to mitochondria under circumstances that promote fission to interact with mitochondrial outer membrane protein fission 1 (Fis1) (22). The balance between mitochondrial fission and fusion is important in maintaining mitochondrial quality. Mitochondrial fusion ensures mixing of organelle components, ensures preservation of mitochondrial membrane potential, protects against oxidant stress and apoptosis, and allows for optimal bioenergetic function (23–27). Conversely, mitochondrial fission is associated with apoptosis (28,29).

Here we report that IHG-1 is a novel regulator of mitochondrial dynamics and bioenergetic function and contributes to cell survival following oxidant stress. These data suggest that IHG-1 plays a pivotal role in maintaining mitochondrial quality, an important feature of TIF in diabetic kidney disease (30).

## RESEARCH DESIGN AND METHODS

### Cell Culture

Stably transduced cell lines have been described previously (Supplementary Fig. 1) (4,6). No significant effects of doxycycline were observed (Supplementary Figs. 2 and 3).

### XF Bioenergetic Assay

Cells were counted and seeded in XF24 culture plates at $7.5 \times 10^4$ cells per well in 100 μL of culture medium. Once cells had attached (~2 h) a further 250 μL of culture medium was added, and cells were incubated at 37°C with 5% $CO_2$ overnight. Prior to assay, cells were washed with assay media (XF assay medium supplemented with 1 mmol/L sodium pyruvate, 1 mg/mL glucose, and 2 mmol/L L-glutamine) and equilibrated in 675 μL prewarmed assay media per well at 37°C with no $CO_2$ for 1 h. Measurements of oxygen consumption rate (OCR) and extracellular acidification rate (ECAR) were performed using an XF24 extracellular flux analyzer (Seahorse Bioscience). Prior to each rate measurement, each sample was gently mixed for 2 min and a further 3-min wait time was used to allow oxygen partial pressure to reach equilibrium. For each rate measurement, OCR and ECAR were measured simultaneously for 3 min. Once a baseline measurement had been established, rates were measured following compound addition (1 μmol/L oligomycin, 0.5 μmol/L carbonyl cyanide 4-(trifluoromethoxy)phenylhydrazone, and 0.1 μmol/L rotenone). At the end of each assay, cell density per well was determined by removing the assay media and adding 2.5 μmol/L calcein-AM in PBS (200 μL per well). Cells were incubated for 1 h at 37°C, and fluorescence intensity at 530 nm (excitation = 488 nm) was the measured using a FLUOstar Omega plate reader. OCR and ECAR measurements were normalized to cell density for each sample.

### ATP Quantification

Cells were seeded in 96-well culture plates at $7.0 \times 10^4$ cells per well in 100 μL of culture medium. Cells were incubated overnight. Intracellular ATP was measured using an ATPlite Luminescence ATP detection kit according to manufacturer's instructions (PerkinElmer). ATP concentration in samples was determined using a standard curve. Cell density for each sample was measured in duplicate wells by removing the culture medium and adding 2.5 μmol/L calcein-AM (Merck) in PBS (200 μL per well). Cells were incubated for 1 h at 37°C, and fluorescence intensity at 530 nm (excitation = 488 nm) was measured using a FLUOstar Omega plate reader. ATP concentration was normalized to cell density for each sample.

### Assessment of Mitochondrial Morphology

Mitochondrial morphology was examined by fluorescence microscopy in cells transduced with pLenti6/AcGFP1-Mito. Cells were cultured on eight-well μ-slides. Andor iQ software was used to acquire images with an Andor Technology iXon$^{EM}$+ EMCCD camera mounted on a Nikon Eclipse Ti microscope equipped with a Yokogawa CSU-X1 scan head using a Nikon Plan Apo 40× oil (NA = 1.3) or Nikon Plan Fluor 100× oil objective (NA = 1) at 37°C in phenol red-free media. Cells were classified based on the majority (>70%) of mitochondria. Tubular network-like morphology with constant diameter throughout the cell was considered *normal*; short/punctuate mitochondria were considered *fragmented*; increased mitochondrial diameter and aggregation of mitochondria was considered *fused*; and continuous tubular mitochondria with very little branching were considered *elongated*. For each sample, 45 individual cells were analyzed, each from a separate field and from at least three independent experiments.

### Fluorescence Recovery After Photobleaching Analysis

For fluorescence recovery after photobleaching (FRAP) analysis, HeLa cells were cultured on eight-well μ-slides. FRAP assessments were carried out using Andor iQ software with an Andor Technology iXon$^{EM}$+ EMCCD camera mounted on a Nikon Eclipse Ti microscope equipped with a Yokogawa CSU-X1 scan using a Nikon Plan Fluor 100× oil objective (NA = 1) at 37°C in phenol red-free media. Mitochondrial-targeted GFP (mtGFP) was bleached to ~50% of the initial signal using a brief pulse of high-intensity laser illumination, followed by acquisition of images every 2 s for duration of 2 min.

### Polyethylene Glycol–Mediated Cell Fusion Assay

This assay was adapted from Legros et al. (31). Cells expressing AcGFP1-Mito and DsRed2-Mito were mixed and plated on eight-well μ-slides 8–16 h before cell fusion. Cells at 70–100% confluency were washed with PBS and incubated for 30 s with 500 μL of a 50% (weight/volume in minimum essential medium) solution of polyethylene glycol (PEG) 1500. Cells were then washed gently three times with prewarmed culture medium containing 20 μg/mL cycloheximide to inhibit protein synthesis.

Imaging of polykaryons containing both GFP- and RFP-labeled mitochondria was commenced 5 h after cell fusion. Images were acquired using Andor iQ software with an Andor Technology iXon$^{EM}$+ EMCCD camera mounted on a Nikon Eclipse Ti microscope equipped with a Yokogawa CSU-X1 scan head using a Nikon Plan Apo 40× oil (NA = 1.3) objective (NA = 1) at 37°C in phenol red-free media. Images were taken at 30-min intervals for at least 5 h. Mitochondrial fusion was determined to have occurred in regions where GFP and RFP were merged (i.e., yellow fluorescence detected due to overlap of fluorophores).

### GTP-Binding Assay

Cells were lysed in lysis buffer (20 mmol/L Tris pH 8.0, 135 mmol/L NaCl, 1 mmol/L $MgCl_2$, 0.1 mmol/L $CaCl_2$, 10% glycerol, 1% NP-40, and 50 mmol/L β–glycerophosphate) supplemented with protease inhibitor cocktail. GTP-agarose beads were blocked in 1% BSA for 1 h at 4°C and then washed twice with wash buffer (25 mmol/L 3-N-morpholinopropanesulfonic acid pH 7.2, 12.5 mmol/L β–glycerophosphate, 25 mmol/L $MgCl_2$, 5 mmol/L EGTA, 2 mmol/L EDTA, 0.002% BSA, and 0.25 mmol/L dithiothreitol). Cell lysates were incubated with blocked GTP-agarose beads for 2 h at 4°C. Samples were then washed three times with lysis buffer. GTP-bound Mfn2 was assessed by immunoblotting. Cell lysate incubated with unbound agarose demonstrates the specificity of the binding (Supplementary Fig. 1*E*).

### Calcium Measurements

Measurement of $[Ca^{2+}]_i$ mobilization was carried out using the Fluoroskan Ascent FL according to a previous method (32).

### Apoptosis Assay and Analysis of Mitochondrial Membrane Potential

Cells at ~80% confluency were treated with glucose oxidase (10 μg/mL) or sorbitol (200 or 250 mmol/L). Cells were detached using Accutase after treatment and combined with floating cells. For assessment of apoptosis, cells were washed and incubated with annexin V-fluorescein isothiocyanate in binding buffer (200 mmol/L HEPES, 2.8 mol/L NaCl, and 50 mmol/L $CaCl_2$) for 15 min at 37°C. Cells were washed once with binding buffer prior to the addition of 10 μg/mL propidium iodide. Cells were then analyzed using a cyan ADP cytometer. For mitochondrial membrane potential measurements, cells were stained with 200 nmol/L tetramethylrhodamine ethyl ester (TMRE) for 15 min or 5 μg/mL JC-1 for 15 min at 37°C. Cells were then washed once with PBS. TMRE was measured at 575 nm and JC-1 at 530 and 590 nm.

### Statistical Analysis

All experiments were carried out with a minimum of $n$ = 3. Intergroup comparisons were made by Student $t$ test or one-way ANOVA followed by Tukey posttest using GraphPad Prism, with $P < 0.05$ considered statistically significant.

## RESULTS

### IHG-1 Is Required for Mitochondrial Respiration

We have previously reported that IHG-1 increases mitochondrial biogenesis and stabilizes the transcriptional activator PGC-1α in both renal proximal tubule cells (RPTC) and HeLa cells (4). PGC-1α activity regulates mitochondrial respiration and functions to boost respiratory capacity to withstand cellular stress, suggesting that IHG-1 may regulate mitochondrial respiration (19). In order to investigate the role of IHG-1 in cellular respiration, we used an extracellular flux analyzer to measure OCR in previously generated stable proximal tubule (HK-2) cell lines expressing tetracycline-inducible IHG-1–specific short hairpin RNA interference (shRNAi) or a scrambled shRNAi control (*Scr*) (4).

Loss of endogenous IHG-1 expression led to a significant decrease in both basal respiration and total respiratory capacity (less than 50% of control cells; $P < 0.01$) (Fig. 1*A*) and a significant decrease in ATP production (Fig. 1*B*). Expression of mitochondrial complexes II and V were unaltered (Fig. 1*C*). Conversely, overexpression of IHG-1 led to a significant increase in both basal respiration and cellular respiratory capacity (Fig. 1*D*). These data indicate that IHG-1 is required for mitochondrial respiration in renal proximal tubules cells.

### IHG-1 Increases Mitochondrial Fusion

Dynamic fusion and fission events are important for the bioenergetic function of mitochondria (18). To assess the role of IHG-1 in mitochondrial dynamics, we fluorescently labeled mitochondria by overexpressing mtGFP in previously generated stable cell lines overexpressing IHG-1 or expressing IHG-1 shRNAi (Supplementary Fig. 1) (4). Mitochondrial networks in these cells were analyzed by confocal microscopy and scored as being normal, fragmented, elongated, or fused (i.e., aggregates principally clustered around the nucleus). Mitochondrial networks in control cells were typically highly connected and contained tubular mitochondria (Fig. 2). Loss of endogenous IHG-1 expression resulted in a marked reduction in mitochondrial connectivity and individual mitochondria that were small and punctate in appearance (Fig. 2*A*). Further images for each cell line are shown in Supplementary Fig. 4. This was not associated with increased turnover of mitochondria (Supplementary Fig. 5). Conversely, overexpression of IHG-1 resulted in mitochondria that were aggregated or fused (Fig. 2*B*). The effects of both IHG-1 knockdown and overexpression were not related to changes in the expression of known mediators of fission or fusion including Drp1, Fis1, Mfn1, Mfn2, and OPA1 (Supplementary Fig. 6).

FRAP was performed on IHG-1 overexpression and knockdown cell lines to quantify mitochondrial dynamics. Reduced endogenous IHG-1 expression resulted in a significant decrease in the rate of fluorescence recovery (expressed as a percentage of the original fluorescence prior to photobleaching), signifying reduced mitochondrial fusion ($P < 0.05$) (Fig. 3*A*), whereas IHG-1 overexpression

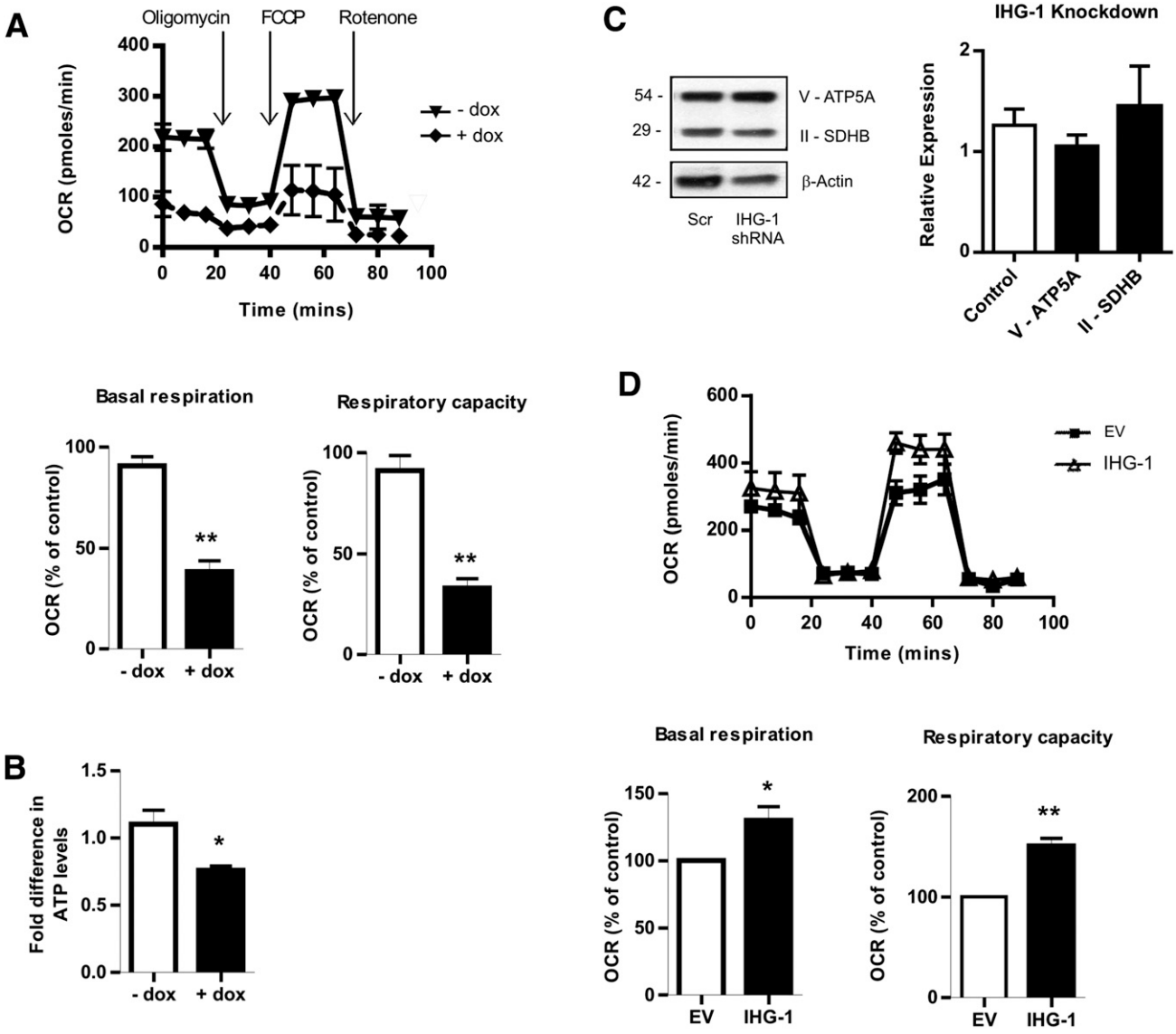


**Figure 1**—IHG-1 is required for mitochondrial respiration. *A*: Human kidney 2 cells expressing tetracycline-inducible shRNAi constructs specific for IHG-1 were cultured in the presence or absence of doxycycline (dox) for 96 h prior to measurement of OCR. Black triangles represent IHG-1 shRNA cell lines –doxycycline; black diamonds represent IHG-1 shRNA cell lines +doxycycline. Basal respiration and respiratory capacity are shown +/−doxycycline. Line plots represent a single experiment in which triplicate wells were analyzed for each cell line and are representative of $n = 4$ (carried out on 4 separate days). Bar charts represent the mean and SEM for $n = 4$. *B*: Intracellular ATP levels were measured in cells from *A*. *C*: Whole-cell lysates from cells in *A* were analyzed by immunoblotting with antibodies specific for complex II (succinate dehydrogenase complex, subunit B, iron sulfur [SDHB]) and complex V (ATP synthase α-subunit) of the mitochondrial electron transport chain. β-Actin antibody binding demonstrates equal protein loading. *D*: Basal respiration and respiratory capacity were determined for human kidney 2 cells stably overexpressing IHG-1 (open triangles) or control cells (empty vector [EV]; black squares) as in *A*. $^*P < 0.05$; $^{**}P < 0.01$; mean ± SEM; $n = 4$ throughout. ATP5A, ATP synthase α-subunit; FCCP, carbonyl cyanide 4-(trifluoromethoxy)phenylhydrazone.

resulted in a significant increase in the rate of fluorescence recovery, indicating increased mitochondrial fusion ($P < 0.05$) (Fig. 3*B*).

To further validate the role of IHG-1 in mitochondrial fusion, a PEG-mediated cell fusion assay was performed. IHG-1 overexpression and knockdown cell lines expressing mitochondrial-targeted RFP (mtRFP) were generated. PEG was used to catalyze the fusion of cellular membranes of the cell lines with RFP- and GFP-labeled mitochondria; this was performed in the presence of cycloheximide to inhibit protein synthesis. Twelve hours after PEG addition, significantly less fluorophore overlap was seen in IHG-1 knockdown cells compared with control cells, indicating a decreased rate of mitochondrial fusion (Fig. 3*C*). Conversely, in cells overexpressing IHG-1, fluorophore overlap was seen to occur at a notably faster rate when compared with control cells, demonstrating an increased rate of mitochondrial fusion (Fig. 3*D*). Further images for each cell

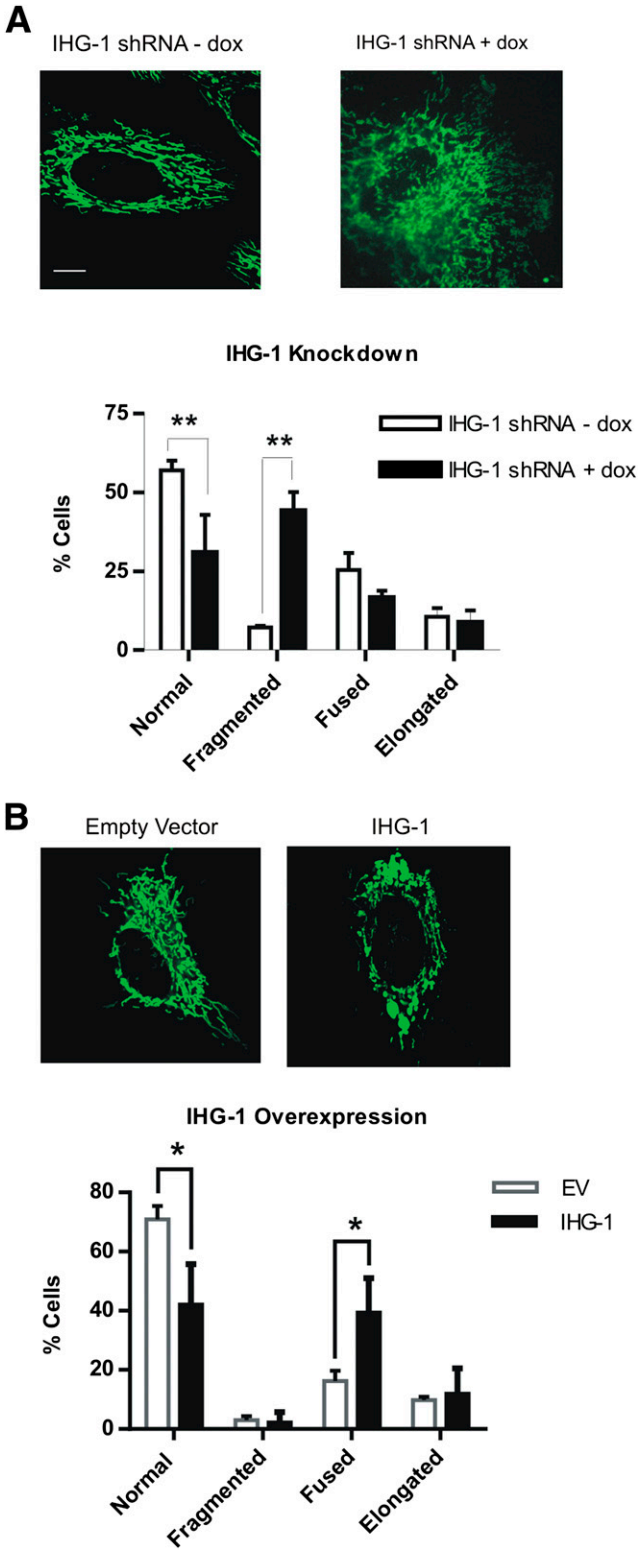


**Figure 2**—Altered expression of IHG-1 results in altered mitochondrial morphology. *A*: HeLa cells expressing tetracycline-inducible shRNAi constructs specific for IHG-1 were transduced with lentiviral vector expressing mtGFP. Cells were then cultured in the absence or presence of doxycycline for 96 h. Representative confocal images of each cell line are shown. Mitochondrial morphology was scored as normal, fragmented, fused, or elongated for at least 15 cells for each per experiment. Graphs present the data as the mean and SEM for three independent experiments ($n$ = 45). *B*: Control HeLa cells (empty vector) or cells stably overexpressing IHG-1 were transduced with lentiviral vector expressing mtGFP and scored as in *A*. Representative confocal images are shown for each cell line. Results are presented graphically as the mean and SEM for four independent experiments ($n$ = 60). Scale bar, 10 μm. $^*P < 0.05$; $^{**}P < 0.01$; mean ± SEM. dox, doxycycline; EV, empty vector.

line are shown in Supplementary Fig. 7. These data strongly indicate that IHG-1 increases mitochondrial fusion.

### IHG-1 Forms a Complex With Mfns

Mfns (Mfn1 or Mfn2) are essential for mitochondrial fusion, while mitochondrial fission relies on Drp1 and Fis1 (20–22). In order to investigate whether IHG-1 interacts with known mediators of mitochondrial dynamics, protein lysates from HEK293 cells transfected with IHG-1-V5 in combination with Mfn1, Mfn2, Drp1 (all FLAG-tagged), or Fis1 (Myc-tagged) were subjected to immunoprecipitation with both V5 and FLAG (or Myc) antibodies. The immunoprecipitated proteins were analyzed by Western blots probed with V5 and either FLAG or Myc antibodies. All proteins were successfully immunoprecipitated. IHG-1 was coimmunoprecipitated with both Mfn1 (Fig. 4*A*) and Mfn2 (Fig. 4*B*) but not with either Drp1 (Fig. 4*C*) or Fis1 (Fig. 4*D*), indicating that IHG-1 and Mfn1 and Mfn2 are protein-protein binding partners. Endogenous IHG-1 and Mfn2 were also confirmed to form a complex by coimmunoprecipitation (Fig. 4*E*). These data demonstrate that IHG-1 forms a complex with both Mfn GTPases.

### IHG-1 Must Complex With Mfn1 and Mfn2 to Increase Mitochondrial Fusion

IHG-1 has an amino terminal mitochondrial targeting sequence that is necessary for its import into mitochondria (4–6). We have previously generated a deletion mutant of IHG-1 that lacks the mitochondrial targeting sequence: Δmts-IHG-1 (6). To investigate whether mitochondrial localization was necessary for IHG-1 to bind to Mfns, HEK293 cells were transfected with Δmts-IHG-1-V5 in combination with FLAG-Mfn1 or FLAG-Mfn2 and subjected to immunoprecipitation with both V5 and FLAG antibodies. Δmts-IHG-1 did not bind to either Mfn1 or Mfn2 (Fig. 5*A*), indicating that IHG-1 must be localized to mitochondria to interact with the Mfns. To investigate whether Δmts-IHG-1 increased mitochondrial fusion, FRAP analysis was performed in a stable cell line expressing Δmts-IHG-1. Δmts-IHG-1 expression resulted in a significant decrease in the rate of fluorescence recovery, indicating decreased mitochondrial fusion (Fig. 5*B*). Therefore, IHG-1 must be localized to mitochondria to interact with Mfn1 and Mfn2 and increase mitochondrial fusion. These data indicate that that IHG-1 must interact with the Mfns to enhance mitochondrial fusion.

### IHG-1–Mfn2 Complex Results in Increased GTP Bound to Mfn2

Mitochondrial fusion requires a functional GTP-binding domain in the Mfns (33). Crystallized IHG-1 was found

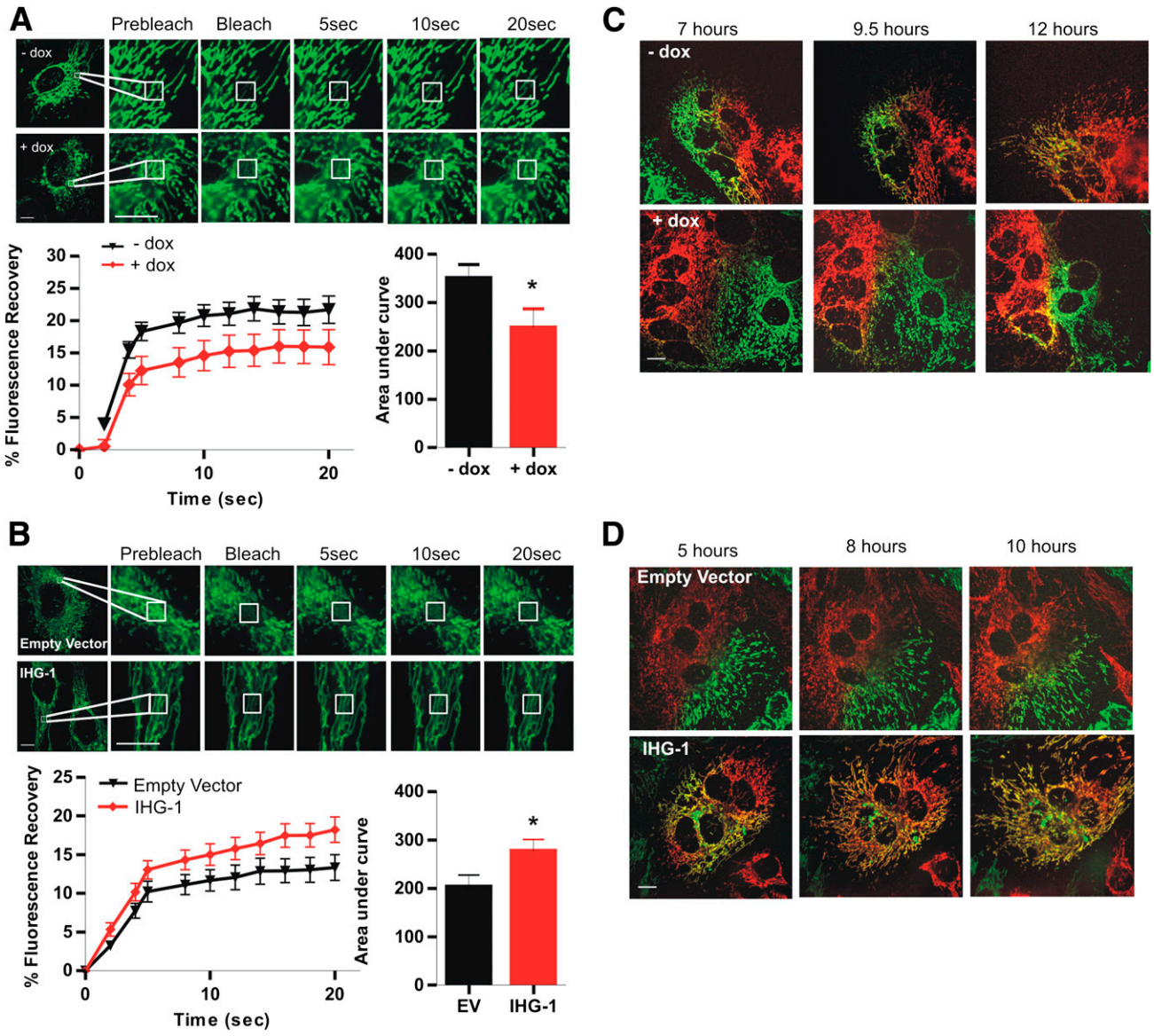


**Figure 3**—IHG-1 increases mitochondrial fusion. *A*: HeLa cells expressing tetracycline-inducible shRNAi constructs specific for IHG-1 were transduced with lentiviral vector expressing mtGFP. (*Top*) Cells were cultured in the presence or absence of doxycycline for 96 h. FRAP assessments were carried out by live cell imaging. (*Bottom*) Fluorescence recovery was analyzed for at least 15 cells for each cell line per experiment. Fluorescence recovery over time is expressed as a percentage of the original fluorescence prior to photobleaching (left-hand panel). For each individual cell assessed, the area under the curve was calculated and is presented in the right-hand panel. Results are presented as the mean and SEM for three independent experiments ($n$ = 45). Scale bar, 10 μm. Black triangles represent IHG-1 shRNA cell lines –doxycycline; red diamonds represent IHG-1 shRNA cell lines +doxycycline. *B*: (*Top*) FRAP assessments were carried out in HeLa cells stably overexpressing either IHG-1 or control cells (empty vector) as in *A*. Results are presented as the mean and SEM for three independent experiments ($n$ = 45). Scale bar, 10 μm. (*Bottom*) Black triangles represent empty vector cell lines; red diamonds represent IHG-1 cell lines. *C*: Cells from *A* were transduced with lentiviral vector expressing either mtGFP or mtRFP. GFP and RFP cells for each cell line were cocultured and fused by incubation with PEG. Mitochondrial fusion, as measured by overlapping RFP and GFP fluorescence, was assessed over 12 h. Representative confocal images for each cell line are shown. Scale bar, 20 μm. *D*: Cells from *B* were transduced with lentiviral vector expressing either mtGFP or mtRFP. Mitochondrial fusion was assessed as in *C* over 10 h. Representative confocal images for each cell line are shown. Scale bar, 20 μm. *$P$ < 0.05; mean ± SEM; $n$ = 3 throughout. dox, doxycycline; EV, empty vector.

bound to GTP (34), suggesting that IHG-1 may possibly increase Mfn activity by increasing GTP binding, i.e., by acting as a guanine nucleotide exchange factor (GEF). Cell lysates from IHG-1 knockdown and overexpression cell lines were incubated with GTP-agarose in order to investigate the ability of IHG-1 to modulate Mfn-GTP binding. GTP-bound Mfn2 was measured by immunoblot and quantified by densitometry. Loss of endogenous IHG-1 expression resulted in a reduction in the amount of GTP bound to Mfn2 (Fig. 6*A*) and reduced mitochondrial fusion (Fig. 3*A* and *C*), while overexpression of IHG-1 led to increased Mfn2-GTP binding (Fig. 6*B*) and increased

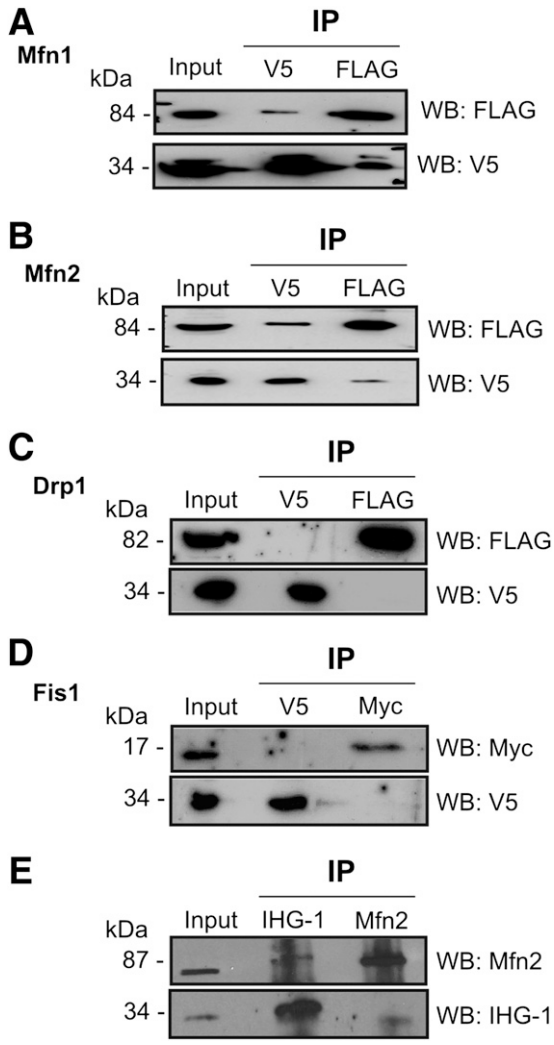


**Figure 4**—IHG-1 binds to Mfn1 and Mfn2. HEK293T cells were cotransfected with IHG-1-V5 and FLAG-tagged Mfn1 (*A*), Mfn2 (*B*), and Drp1 (*C*) or Myc-tagged mitochondrial Fis1 (*D*). Binding of proteins was assessed by immunoprecipitation and Western blotting (WB). *E*: Endogenous IHG-1 or Mfn2 was immunoprecipitated from HeLa cells. Coimmunoprecipitation of the alternate protein was assessed by Western blotting. IP, immunoprecipitation.

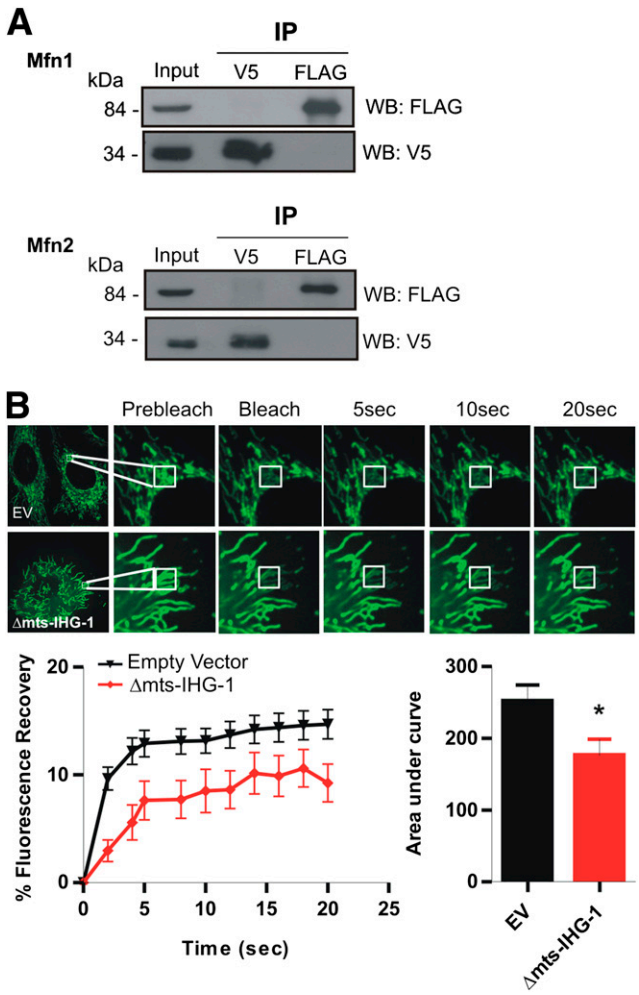


**Figure 5**—IHG-1 must complex with Mfn1 and Mfn2 to increase mitochondrial fusion. *A*: HEK293T cells were cotransfected with Δmts-IHG-1-V5 and either FLAG-tagged Mfn1 or Mfn2. Binding of proteins was assessed by immunoprecipitation and Western blotting (WB). *B*: (*Top*) FRAP assessments were carried out in HeLa cells stably overexpressing Δmts-IHG-1 or control cells (empty vector) that were transduced with lentiviral vector expressing mito-GFP. Presentation and analyses of results are as described in Fig. 3*A*. (*Bottom*) Black triangles represent empty vector cell lines; red diamonds represent Δmts-IHG-1 cell lines. $^*P < 0.05$; mean ± SEM; $n = 3$ throughout. IP, immunoprecipitation; EV, empty vector.

mitochondrial fusion (Fig. 3*B* and *D*). IHG-1 must complex with Mfn2 to increase GTP binding, as overexpression of Δmts-IHG-1 resulted in a reduction in the amount of GTP bound to Mfn2 (Fig. 6*B*) and reduced mitochondrial fusion (Fig. 5*B*). These data indicate that IHG-1 increases GTP-bound Mfn2, suggesting that IHG-1 may function as a GEF and thus enhance mitochondrial fusion.

### IHG-1 Does Not Alter Calcium Levels

Lack of MFN2 has been shown to lead to increased calcium release from endoplasmic reticulum (ER) stores following stimulation with the sarcoplasmic-ER $Ca^{2+}$ ATPase inhibitor tert-buthyl benzohydroquinone (tBuBHQ) (35). tBuBHQ causes the passive release of $Ca^{2+}$ from ER stores, resulting in increases in cytosolic $Ca^{2+}$ concentration ($[Ca^{2+}]_i$). The increase in cytosolic calcium when measured with the fluorescent dye Fluo-4/AM was similar in IHG-1 overexpressing, IHG-1 shRNA knockdown, and control HeLa cell lines (Fig. 7). These data indicate that IHG-1 does not alter cytosolic calcium.

### Increased IHG-1 Expression Protects Cells From ROS-Induced Apoptosis

Mitochondrial production of ROS is proposed as the primary event leading to development of diabetic vascular complications (8). Increased mitochondrial fusion decreases ROS production (12,27) and is an important process for maintenance of mitochondrial quality (36). IHG-1 may function in the diabetic kidney to preserve mitochondrial function following oxidant stress. To investigate the role

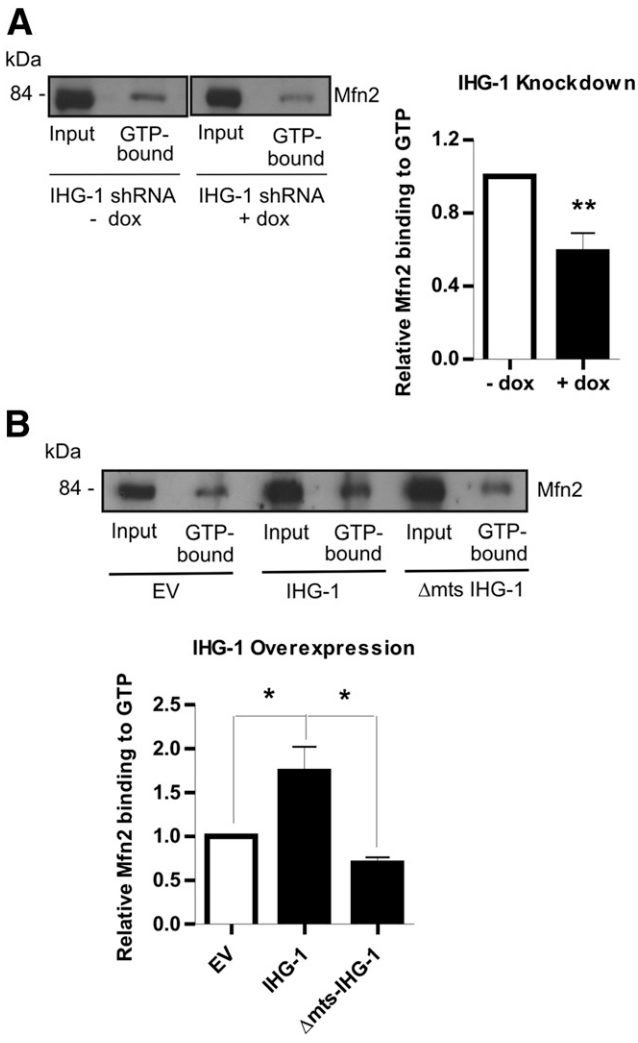


**Figure 6**—IHG-1 increases Mfn2-GTP binding. *A*: HeLa cells expressing tetracycline-inducible shRNAi constructs specific for IHG-1 or a scrambled construct (Scr) were cultured in the presence of doxycycline for 96 h. Whole-cell lysates were incubated with GTP-agarose beads for 2 h. GTP-bound Mfn2 was assessed by Western blotting. The percentage of Mfn2 bound to GTP was calculated based on input samples and is presented as the mean and SEM (right-hand panel). *B*: Whole-cell lysates from HEK293T cells transfected with V5-tagged IHG-1, Δmts-IHG-1, or control cells (empty vector) were assayed as in *A*. $^{*}P < 0.05$; $^{**}P < 0.01$; $n = 3$ throughout. dox, doxycycline; EV, empty vector.

of IHG-1 in cell survival following oxidative stress, IHG-1 overexpressing cell lines were treated with glucose oxidase, which catalyzes the oxidation of glucose to hydrogen peroxide. IHG-1 overexpression significantly protected the cells from ROS-induced apoptosis (Fig. 8*A*) and resulted in a significant preservation of mitochondrial membrane potential as demonstrated by TMRE staining (Fig. 8*B*) and confirmed by JC-1 staining (Supplementary Fig. 8). These data indicate that IHG-1 plays an important role in maintaining mitochondria function and cell viability following oxidant stress. No protective effect against hyperosmotic stress-induced apoptosis was seen following overexpression of IHG-1 (Fig. 8*C*), suggesting that the antiapoptotic effects of IHG-1 may be limited to ROS.

## DISCUSSION

In this article, we propose IHG-1 as a novel regulator in the mitochondrial quality control axis and a key element in the cellular response to oxidant stress. In diabetes, hyperglycemia has damaging effects on mitochondria, resulting in the accumulation of dysfunctional mitochondria and ultimately organ damage (7,37). Mitochondrial quality control relies on maintaining balanced mitochondrial biogenesis, fusion, and fission (7,37,38). Increased stress (e.g., oxidative stress) can alter this balance, leading to dysfunctional mitochondria and disease. Hyperglycemia-induced mitochondrial production of ROS plays a critical role in disease development (9) and disease-associated TGF-β1 activity (10) in the diabetic kidney.

We have previously reported mitochondrial IHG-1 to amplify TGF-β1 signaling, stabilize PGC-1α protein, and increase mitochondrial biogenesis in kidney cells (4–6). IHG-1 both increases and prolongs phosphorylation of TGF-β1 signaling mediator Smad3, which, in turn, has been reported to regulate mitochondrial biogenesis (14,17). Consistent with IHG-1–induced stabilization of PGC-1α, we report here that IHG-1 is necessary for mitochondrial respiration. PGC-1α was originally believed essential for mitochondrial biogenesis, but recent studies indicate its principal role is to regulate mitochondrial respiration and to boost respiratory capacity to withstand stress (19). Our data indicate that IHG-1 is necessary for mitochondrial respiratory function in RPTC.

Balanced mitochondrial fusion and fission are critical in maintaining mitochondrial quality (24,37). The rates of fusion and fission need to be tightly controlled to adapt to varying bioenergetic demands in changing physiological conditions (37). Dysregulation of mitochondrial dynamics is a feature of diabetic disease (7,13,37,39,40). IHG-1 increases mitochondrial fusion, consistent with the role of IHG-1 in oxidative phosphorylation and mitochondrial biogenesis. Increased IHG-1 expression leading to increased mitochondrial fusion may be a recovery mechanism in response to hyperglycemic stress. Sustained hyperglycemic insult and resulting persistent increases in IHG-1 expression would lead to enhanced mitochondrial fusion and biogenesis, Smad3 signaling, and fibrosis.

Hyperglycemia has been described to induce mitochondrial fission in pancreatic β-cells (39), liver cells (13), endothelial cells, and podocytes (40). However, as adaption of mitochondrial bioenergetic capacity to nutrient availability differs among tissues, the differing responses are likely due to specific cellular physiology. It is worth noting that previous reported studies investigating hyperglycemic-induced changes in mitochondrial dynamics focused on acute exposure to high extracellular glucose (i.e., between 15 min and 48 h) (13,39,40). Monitoring of mitochondrial dynamics throughout the 48-h period showed fluctuating cycles of fission associated with ROS

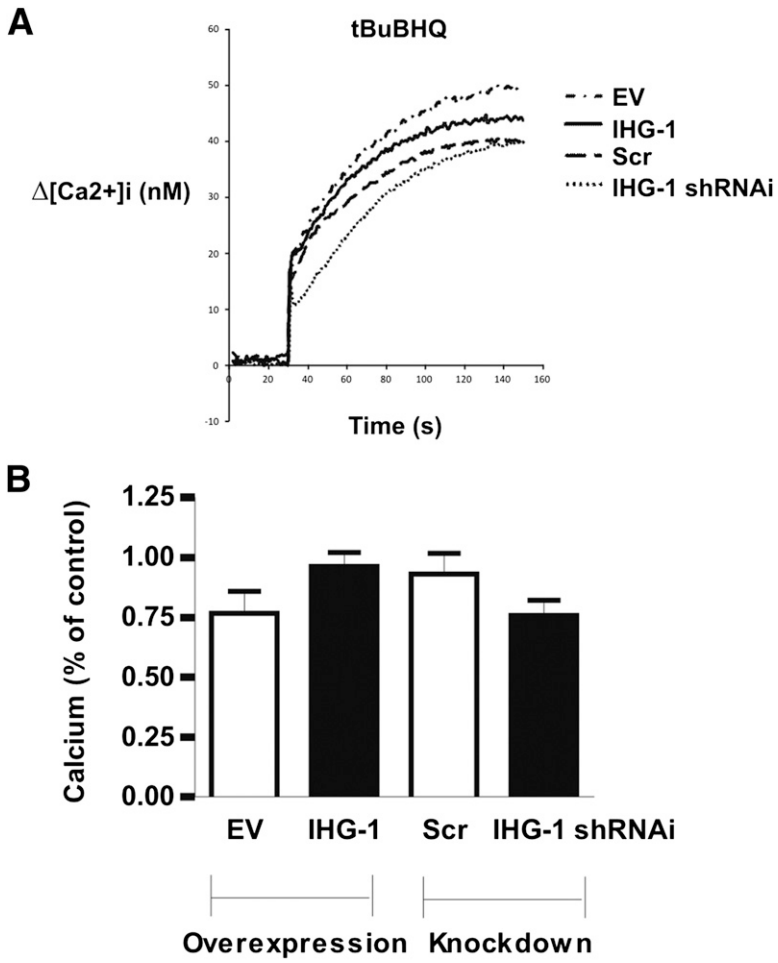


**Figure 7**—IHG-1 does not alter $Ca^{2+}$ levels. *A*: Representative recordings of $[Ca^{2+}]_i$ mobilization after passive discharge of ER $Ca^{2+}$ stores by tBuBHQ (0.5 mmol/L) in HeLa cell lines expressing IHG-1 or shRNAi constructs specific for IHG-1 and in control (empty vector) and Scr cell lines. *B*: Bar graph represents the mean and SEM for three independent experiments. There was no significant difference in means. EV, empty vector.

production followed by restoration of mitochondrial architecture (and loss of ROS) (13). These data suggest that in hyperglycemic conditions, increased mitochondrial fission (either resulting from or contributing to increased ROS production) initiates pathways that increase mitochondrial fusion in a cyclic fashion in order to restore the imbalance in mitochondrial dynamics. Therefore, it seems probable that sustained exposure to hyperglycemia may result in imbalanced mitochondrial dynamics, possibly ultimately resulting in increased mitochondrial fusion in RPTC and possibly other cell types.

This concept is strengthened by the observation that in early stages of diabetic kidney disease in streptozotocin-induced diabetic rats, ultrastructural changes in mitochondria in RPTC (described as giant mitochondria) were found to correlate with disturbances in the main functions of renal tubule cells and typical features of DN (41). Electron microscopy studies have shown that the mean size of mitochondria was larger in DN compared with those in normal controls (41). Similar findings were described for mitochondria in RPTC of streptozotocin-induced diabetic mice (42). Increased IHG-1 expression, leading to increased mitochondrial fusion, may be a recovery mechanism in response to hyperglycemic stress. Sustained hyperglycemic insult and resulting persistent increases in IHG-1 expression would lead to enhanced mitochondrial fusion and biogenesis, Smad3 signaling, and fibrosis.

Hyperglycemia-induced mitochondrial ROS production is a critical mediator in the development and progression of diabetic vascular complications (8). Increased ROS levels are deleterious to cells and lead to increased mitochondrial fragmentation and apoptosis (43–45), while mitochondrial fusion protects cells from apoptosis (27). IHG-1 overexpression protected cells from ROS-induced apoptosis consistent with its ability to increase mitochondrial fusion.

IHG-1 protects cells from oxidant stress and may function in the diabetic kidney to preserve mitochondrial function and cell viability, while at the same time amplifying TGF-β profibrotic responses. Prosurvival signals are critical in dedifferentiation of RPTC following oxidation injury (46). Dedifferentiation of RPTC is one of the major pathways leading to TIF. The survival of

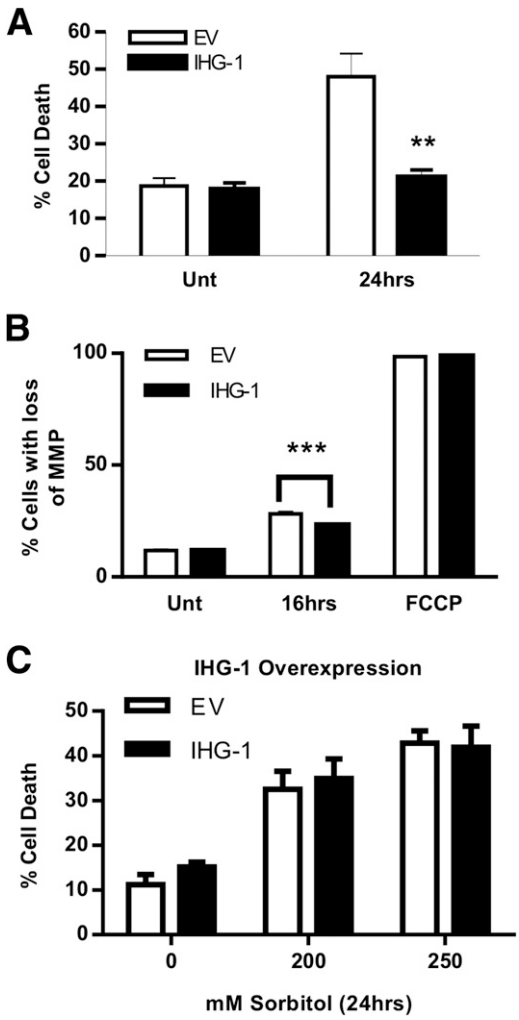


**Figure 8**—IHG-1 protects cells from apoptosis. HeLa cells stably overexpressing IHG-1 or control cells (empty vector) were treated with 10 mU/mL glucose oxidase. *A*: Apoptotic cells were detected at 24 h by annexin V/PI staining and analysis by flow cytometry. *B*: Mitochondrial membrane potential was assessed at 16 h using TMRE staining and flow cytometric analysis. *C*: HeLa cells stably overexpressing IHG-1 or control cells (empty vector) were treated with the indicated concentrations of sorbitol. Apoptotic cells were detected at 24 h by annexin V/PI staining and analysis by flow cytometry. $^{**}P < 0.01$; $^{***}P < 0.001$; mean ± SEM; $n = 3$ throughout. EV, empty vector; MMP, mitochondrial membrane potential.

damaged epithelial cells is not necessarily beneficial, and the repair of damaged epithelium is frequently maladaptive, resulting in fibrosis, which has major clinical consequences (47,48). TGF-β1, believed to be the key driver of fibrosis in TIF, has been shown to induce mitochondrial fusion in epithelial cells (15).

IHG-1 must complex with Mfn1 and Mfn2 to increase mitochondrial fusion possibly by acting as a GEF. Lack of Mfn2 has been shown to lead to increased calcium release from ER stores as a result of disruption of ER morphology and ER-mitochondrial interaction. While IHG-1 increases Mfn2 activity and possibly enhances ER-mitochondrial interaction, it does not alter calcium release from ER stores.

Mfn2 is an important mediator in response to metabolic stress in the kidney. Murine kidneys were able to maintain normal filtration and tubular function following conditional deletion of Mfn2, yet showed an increased susceptibility to apoptosis following metabolic stress (49). Consistent with the role of mitochondrial fusion in bioenergetic function, Mfn2 has been reported to stimulate respiration, substrate oxidation, and the expression of subunits involved in respiratory complexes (18,50) and is essential for normal glucose homeostasis (51). IHG-1 interaction with Mfn2 therefore may be important not only in increasing mitochondrial fusion, but also in increasing cellular respiratory capacity.

IHG-1 most likely increases mitochondrial fusion by enhancing the GTP-binding capacity of Mfn2, an action independent of its role in amplifying TGF-β1 signaling responses, consistent with the fact that IHG-1 is a more evolutionary ancient protein than TGF-β1. As TGF-β1 also contributes to mitochondrial fusion, the increased expression of both proteins in diabetic kidney disease is likely to be additive; however, neither IHG-1 nor TGF-β1 altered the expression of Mfn2, Drp1, or complexes of the electron transport chain in RPTC (Supplementary Fig. 9).

The function of the core components of mitochondrial dynamics (i.e., FZO/Mfn, Mgm1/EAT-3/OPA1, and Dnm1/DRP1) are highly conserved in yeast, worms, flies, and mammals while regulatory proteins in general are more varied among these organisms (52). IHG-1, similarly, is a highly conserved protein among eukaryotes (5). The IHG-1 yeast homolog THG1 is an essential protein in yeast (34). Therefore, it seems probable that IHG-1 is a core component of the mitochondrial fusion machinery.

In conclusion, we propose IHG-1 as a novel player in the mitochondrial quality control axis. IHG-1 acts to preserve mitochondrial function by coordinating a prosurvival program involving stabilization of PGC-1α protein and increasing mitochondrial respiratory capacity, biogenesis, and fusion. The net result of these actions protects cell viability following oxidative stress but also leads to amplification of profibrotic TGF-β1 activity in RPTC, most likely leading to TIF. IHG-1, like the Mfns, is evolutionarily ancient and remarkably conserved. As IHG-1 must interact with the Mfns to increase fusion and is an essential protein in yeast, it is likely a crucial player in mitochondrial dynamics and quality control.

**Acknowledgments.** The authors thank Dr. Dimitri Scholz and Dr. Alfonso Blanco (University College Dublin, Ireland) for technical assistance with fluorescence microscopy and flow cytometry in this study. The authors are grateful to Dr. Ruth Gimeno (BioTx Pfizer, Cambridge, MA) for IHG-1 antibody and Didier Trono (University of Geneva, Switzerland) for pCMVΔR8.9 and pMD.2G constructs.

**Funding.** This work was funded by Science Foundation Ireland (grant numbers SFI/06/IN.1/B114 and SFI/RFP06/BIC304), Wellcome Trust (grant number 073310/Z/03/Z), the Health Research Board, and the Government of Ireland Programme for Research in Third Level Institutions.

**Duality of Interest.** No potential conflicts of interest relevant to this article were reported.

**Author Contributions.** F.B.H. designed and performed research, analyzed data, and wrote the manuscript. J.B.C. designed and performed research and analyzed data. B.G., U.B., H.M.R., D.A., S.B., and F.F. performed research. H.M. contributed new analytical tools. F.M., C.G., and M.M. designed research, analyzed data, and wrote the manuscript. F.B.H. is the guarantor of this work and, as such, had full access to all the data in the study and takes responsibility for the integrity of the data and the accuracy of the data analysis.

**Prior Presentation.** This work was presented in part at the American Society of Nephrology Annual Meeting, Philadelphia, PA, 8–13 November 2011; the Irish Nephrology Society Meeting, Dublin, Ireland, 13 May 2010; the Irish Cytometry Society Meeting, Dublin, Ireland, 17–18 November 2009; and the Irish Cytometry Society Meeting, Dublin, Ireland, 17–18 November 2010.

## References

1. Murphy M, Godson C, Cannon S, et al. Suppression subtractive hybridization identifies high glucose levels as a stimulus for expression of connective tissue growth factor and other genes in human mesangial cells. J Biol Chem 1999;274:5830–5834
2. Murphy M, Hickey F, Godson C. IHG-1 amplifies TGF-β1 signalling and mitochondrial biogenesis and is increased in diabetic kidney disease. Curr Opin Nephrol Hypertens 2013;22:77–84
3. Clarkson MR, Murphy M, Gupta S, et al. High glucose-altered gene expression in mesangial cells. Actin-regulatory protein gene expression is triggered by oxidative stress and cytoskeletal disassembly. J Biol Chem 2002;277:9707–9712
4. Hickey FB, Corcoran JB, Docherty NG, et al. IHG-1 promotes mitochondrial biogenesis by stabilizing PGC-1α. J Am Soc Nephrol 2011;22:1475–1485
5. Murphy M, Docherty NG, Griffin B, et al. IHG-1 amplifies TGF-beta1 signaling and is increased in renal fibrosis. J Am Soc Nephrol 2008;19:1672–1680
6. Corcoran JB, McCarthy S, Griffin B, et al. IHG-1 must be localised to mitochondria to decrease Smad7 expression and amplify TGF-β1-induced fibrotic responses. Biochim Biophys Acta 2013;1833:1969–1978
7. Liesa M, Shirihai OS. Mitochondrial dynamics in the regulation of nutrient utilization and energy expenditure. Cell Metab 2013;17:491–506
8. Brownlee M. The pathobiology of diabetic complications: a unifying mechanism. Diabetes 2005;54:1615–1625
9. Coughlan MT, Thorburn DR, Penfold SA, et al. RAGE-induced cytosolic ROS promote mitochondrial superoxide generation in diabetes. J Am Soc Nephrol 2009;20:742–752
10. Forbes JM, Coughlan MT, Cooper ME. Oxidative stress as a major culprit in kidney disease in diabetes. Diabetes 2008;57:1446–1454
11. Rasbach KA, Schnellmann RG. Signaling of mitochondrial biogenesis following oxidant injury. J Biol Chem 2007;282:2355–2362
12. Yoon YS, Yoon DS, Lim IK, et al. Formation of elongated giant mitochondria in DFO-induced cellular senescence: involvement of enhanced fusion process through modulation of Fis1. J Cell Physiol 2006;209:468–480
13. Yu T, Robotham JL, Yoon Y. Increased production of reactive oxygen species in hyperglycemic conditions requires dynamic change of mitochondrial morphology. Proc Natl Acad Sci U S A 2006;103:2653–2658
14. Ge X, Vajjala A, McFarlane C, Wahli W, Sharma M, Kambadur R. Lack of Smad3 signaling leads to impaired skeletal muscle regeneration. Am J Physiol Endocrinol Metab 2012;303:E90–E102
15. Ryu SW, Yoon J, Yim N, Choi K, Choi C. Downregulation of OPA3 is responsible for transforming growth factor-β-induced mitochondrial elongation and F-actin rearrangement in retinal pigment epithelial ARPE-19 cells. PLoS ONE 2013;8:e63495
16. Stieger N, Worthmann K, Teng B, et al. Impact of high glucose and transforming growth factor-β on bioenergetic profiles in podocytes. Metabolism 2012;61:1073–1086
17. Yadav H, Quijano C, Kamaraju AK, et al. Protection from obesity and diabetes by blockade of TGF-β/Smad3 signaling. Cell Metab 2011;14:67–79
18. Zorzano A, Liesa M, Sebastián D, Segalés J, Palacín M. Mitochondrial fusion proteins: dual regulators of morphology and metabolism. Semin Cell Dev Biol 2010;21:566–574
19. Rowe GC, Patten IS, Zsengeller ZK, et al. Disconnecting mitochondrial content from respiratory chain capacity in PGC-1-deficient skeletal muscle. Cell Reports 2013;3:1449–1456
20. Fritz S, Rapaport D, Klanner E, Neupert W, Westermann B. Connection of the mitochondrial outer and inner membranes by Fzo1 is critical for organellar fusion. J Cell Biol 2001;152:683–692
21. Eura Y, Ishihara N, Yokota S, Mihara K. Two mitofusin proteins, mammalian homologues of FZO, with distinct functions are both required for mitochondrial fusion. J Biochem 2003;134:333–344
22. Yoon Y, Krueger EW, Oswald BJ, McNiven MA. The mitochondrial protein hFis1 regulates mitochondrial fission in mammalian cells through an interaction with the dynamin-like protein DLP1. Mol Cell Biol 2003;23:5409–5420
23. Sugioka R, Shimizu S, Tsujimoto Y. Fzo1, a protein involved in mitochondrial fusion, inhibits apoptosis. J Biol Chem 2004;279:52726–52734
24. Sesaki H, Jensen RE. Division versus fusion: Dnm1p and Fzo1p antagonistically regulate mitochondrial shape. J Cell Biol 1999;147:699–706
25. Song Z, Ghochani M, McCaffery JM, Frey TG, Chan DC. Mitofusins and OPA1 mediate sequential steps in mitochondrial membrane fusion. Mol Biol Cell 2009;20:3525–3532
26. Anne Stetler R, Leak RK, Gao Y, Chen J. The dynamics of the mitochondrial organelle as a potential therapeutic target. J Cereb Blood Flow Metab 2013;33:22–32
27. Gomes LC, Di Benedetto G, Scorrano L. During autophagy mitochondria elongate, are spared from degradation and sustain cell viability. Nat Cell Biol 2011;13:589–598
28. Neuspiel M, Zunino R, Gangaraju S, Rippstein P, McBride H. Activated mitofusin 2 signals mitochondrial fusion, interferes with Bax activation, and reduces susceptibility to radical induced depolarization. J Biol Chem 2005;280:25060–25070
29. Twig G, Elorza A, Molina AJ, et al. Fission and selective fusion govern mitochondrial segregation and elimination by autophagy. EMBO J 2008;27:433–446
30. Weinberg JM. Mitochondrial biogenesis in kidney disease. J Am Soc Nephrol 2011;22:431–436
31. Legros F, Lombès A, Frachon P, Rojo M. Mitochondrial fusion in human cells is efficient, requires the inner membrane potential, and is mediated by mitofusins. Mol Biol Cell 2002;13:4343–4354
32. Lin K, Sadée W, Quillan JM. Rapid measurements of intracellular calcium using a fluorescence plate reader. Biotechniques 1999;26:318–322, 324–326
33. Chen H, Detmer SA, Ewald AJ, Griffin EE, Fraser SE, Chan DC. Mitofusins Mfn1 and Mfn2 coordinately regulate mitochondrial fusion and are essential for embryonic development. J Cell Biol 2003;160:189–200
34. Heinemann IU, Nakamura A, O'Donoghue P, Eiler D, Söll D. tRNAHis-guanylyltransferase establishes tRNAHis identity. Nucleic Acids Res 2012;40:333–344
35. de Brito OM, Scorrano L. Mitofusin 2 tethers endoplasmic reticulum to mitochondria. Nature 2008;456:605–610
36. Miller MW, Knaub LA, Olivera-Fragoso LF, et al. Nitric oxide regulates vascular adaptive mitochondrial dynamics. Am J Physiol Heart Circ Physiol 2013;304:H1624–H1633
37. Westermann B. Mitochondrial fusion and fission in cell life and death. Nat Rev Mol Cell Biol 2010;11:872–884
38. Twig G, Hyde B, Shirihai OS. Mitochondrial fusion, fission and autophagy as a quality control axis: the bioenergetic view. Biochim Biophys Acta 2008;1777:1092–1097
39. Molina AJ, Wikstrom JD, Stiles L, et al. Mitochondrial networking protects beta-cells from nutrient-induced apoptosis. Diabetes 2009;58:2303–2315

40. Wang W, Wang Y, Long J, et al. Mitochondrial fission triggered by hyperglycemia is mediated by ROCK1 activation in podocytes and endothelial cells. Cell Metab 2012;15:186–200
41. Kaneda K, Iwao J, Sakata N, Takebayashi S. Correlation between mitochondrial enlargement in renal proximal tubules and microalbuminuria in rats with early streptozotocin-induced diabetes. Acta Pathol Jpn 1992;42: 855–860
42. Galloway CA, Lee H, Nejjar S, et al. Transgenic control of mitochondrial fission induces mitochondrial uncoupling and relieves diabetic oxidative stress. Diabetes 2012;61:2093–2104
43. Jabs T. Reactive oxygen intermediates as mediators of programmed cell death in plants and animals. Biochem Pharmacol 1999;57:231–245
44. Lee YJ, Cho HN, Soh JW, et al. Oxidative stress-induced apoptosis is mediated by ERK1/2 phosphorylation. Exp Cell Res 2003;291:251–266
45. Macip S, Igarashi M, Berggren P, Yu J, Lee SW, Aaronson SA. Influence of induced reactive oxygen species in p53-mediated cell fate decisions. Mol Cell Biol 2003;23:8576–8585
46. Zhuang S, Yan Y, Han J, Schnellmann RG. p38 kinase-mediated transactivation of the epidermal growth factor receptor is required for dedifferentiation of renal epithelial cells after oxidant injury. J Biol Chem 2005;280:21036–21042
47. Coca SG, Yusuf B, Shlipak MG, Garg AX, Parikh CR. Long-term risk of mortality and other adverse outcomes after acute kidney injury: a systematic review and meta-analysis. Am J Kidney Dis 2009;53:961–973
48. Bonventre JV, Yang L. Cellular pathophysiology of ischemic acute kidney injury. J Clin Invest 2011;121:4210–4221
49. Gall JM, Wang Z, Liesa M, et al. Role of mitofusin 2 in the renal stress response. PLoS ONE 2012;7:e31074
50. Pich S, Bach D, Briones P, et al. The Charcot-Marie-Tooth type 2A gene product, Mfn2, up-regulates fuel oxidation through expression of OXPHOS system. Hum Mol Genet 2005;14:1405–1415
51. Sebastián D, Hernández-Alvarez MI, Segalés J, et al. Mitofusin 2 (Mfn2) links mitochondrial and endoplasmic reticulum function with insulin signaling and is essential for normal glucose homeostasis. Proc Natl Acad Sci U S A 2012; 109:5523–5528
52. Westermann B. Mitochondrial dynamics in model organisms: what yeasts, worms and flies have taught us about fusion and fission of mitochondria. Semin Cell Dev Biol 2010;21:542–549